Near-second-order transition in confined living-polymer solutions

Korobko, Alexander V.; Besseling, Nicolaas A M

DOI
10.1103/PhysRevE.93.032507

Publication date
2016

Document Version
Final published version

Published in
Physical Review E (Statistical, Nonlinear, and Soft Matter Physics)

Near-second-order transition in confined living-polymer solutions

Alexander V. Korobko* and Nicolaas A. M. Besseling
Department of Chemical Engineering, Delft University of Technology, Julianalaan 136, 2628 BL Delft, The Netherlands
(Received 24 November 2015; published 28 March 2016)

We analyze a near-second-order transition occurring in solutions of living polymers confined by two parallel surfaces in equilibrium with a reservoir solution. The molecular self-consistent field theory in the regime of weak adsorption or depletion is mapped to phenomenological Landau theory, where the order parameter is the average degree of polymerization or, equivalently, the normalized chain-end concentration. The distance between two surfaces at which the transition occurs scales as $\ell_c^2|c|$ where ℓ_c is the correlation length of the polymer solution in the reservoir and c^{-1} is de Gennes adsorption length. In the second half of the paper we focus on experimentally observable features. The predicted transition can be detected experimentally by probing the living-polymer mediated disjoining potential between surfaces by means of, e.g., colloidal probe atomic force microscopy. To facilitate experimental investigations we derive simple explicit expressions for the disjoining potential for several regimes. By comparison with full numerical calculations it was verified that these are quite accurate.

DOI: 10.1103/PhysRevE.93.032507

I. INTRODUCTION

Recently, we published on the equilibrium behavior of living polymers confined between two adsorbing surfaces while the confined solution is at equilibrium with a reservoir at constant chemical potential [1]. We predicted the occurrence of a transition at which several relevant properties change dramatically upon a small change of control parameters. In the present paper we clarify the nature of this transition, relating it to the general theory for phase transitions in confined systems. The theory of boundary critical phenomena was developed to explore the effect of surfaces on binary alloys and magnets [2,3]. The phase separation in binary liquids [4] and the transition temperature of superconducting thin films [5] are analogous as well. For all these cases, the transition can be analyzed in terms of the Landau theory [6], which yields the Ginsburg-Landau equation for the order parameter. For thin films with a thickness D, the transition temperature shifts from its value in the bulk by $2\xi^2 c/D$, where ξ is the correlation length and c^{-1} the extrapolation length of the de Gennes boundary condition [7]. We address the analogy between the transition occurring in confined living polymer solutions and the phase transitions in the above-mentioned confined solid-state systems. We show that for the living-polymer case a Landau potential can be deduced from our "molecular-model-based" theoretical analysis [1,8–10]. Comparing this potential with the usual expressions for the Landau potential, we see that in the living-polymer system the role of the reduced temperature is played by a parameter quantifying the nonideality of the living-polymer solution. Interestingly, from the molecular theory for living polymers a term arises in the Landau potential, which corresponds to a negative field contribution. Due to this term there is no true second-order transition, but a weakened transition that we denote "near-second order." In this paper we show furthermore that, somewhat unexpectedly, the transition is not limited to living-polymer solutions confined between *adsorbing* surfaces, but that the conditions at which it occurs extend into the depletion regime, occurring when the surfaces are nonadsorbing towards the polymers.

Living polymers, often called *supramolecular polymers* or *dynamic polymers* [11–14], are chains of segments connected by reversible interactions [11,12]. Bonds between the monomers that form such chains are formed and broken continuously. In bulk solutions, the equilibrium chain-length distribution of living polymers follows a simple exponential law [15], and the number average degree of polymerization, $\langle N\rangle$, of such chains is controlled by the monomer concentration ρ and the equilibrium constant for binding, K_b: $\langle N\rangle \propto \sqrt{\rho K_b}$. To mention some "classical" examples belonging to this class of soft matter we may refer to actin [16], liquid sulfur [17], and wormlike micelles [18,19]. Understanding the behavior of living polymers is getting more urgent as modern supramolecular chemistry is creating many new examples [11,20]. Statistical properties of living-polymer solutions subject to confinement by two parallel surfaces deviate from bulk solutions. Varying the surface-segment affinity from strongly adsorbing to completely depleting, we change the local concentration inside the confined film. For (nearly) ideal polymer solutions confined by two adsorbing surfaces this transition has symptoms of a second-order transition [1,10]. The origin of this behavior lies in the synergy between the local segment density and the degree of polymerization inside a confined film at equilibrium with a reservoir.

For fluid living-polymer solutions experimental methods are available that cannot be used with the above-mentioned solid-state systems. The influence of the confining surfaces upon the confined solutions is reflected in the effective interaction between those surfaces [1,21–24]. Such surface interactions, and how they vary upon variation of the separation between the surfaces, can be probed experimentally by techniques such as surface-force balance methods or colloidal probe atomic force microscopy (CP AFM) [25,26]. The second part of this paper focuses on these experimentally accessible consequences of the above-mentioned transition.

II. NEAR-SECOND-ORDER TRANSITION

The theory starts from an expression for the grand potential, $\Omega = F - \mu n$, for a living-polymer solution confined by two

*korobko.sasha@gmail.com

parallel surfaces with area A. A is taken to be so large that edge effects can be neglected. Here, F denotes the free energy, μ is the chemical potential of the monomers, and n is the total number of monomers. Defining the z axis as normal to the surfaces, the latter are located at $z = 0$ and $z = D$ [8]. The grand potential is written as a functional of the density of chains, $\rho_N(\mathbf{z}^{(N)})$, with degree of polymerization N and "configuration" $\mathbf{z}^{(N)}$, where the "configuration" is defined by all z positions of chain segments. The Euler-Lagrange equation $\partial\Omega/\partial\rho_N(\mathbf{z}^{(N)}) = 0$ can be rewritten as the Laplace-transformed Edwards equation [1,8–10],

$$R_0^2 \frac{d^2 g(z)}{dz^2} = x g(z)^3 + (1-x) g(z) - 1, \tag{1}$$

for the order-parameter profile $g(z)$. Here $R_0 = b\sqrt{\langle N\rangle_0/6}$ is the radius of gyration of an unperturbed coil with degree of polymerization $\langle N\rangle_0$. Here b is the mean-square segment length and $\langle N\rangle_0$ is the number-average degree of polymerization in the reservoir. Parameter $x = \upsilon\rho_0\langle N\rangle_0$, where υ is the excluded-volume parameter and ρ_0 the concentration of segments in the reservoir, measures nonideality of the solution; $x = 0$ defines ideal solutions [10]; and at $x \gtrsim 1$ excluded-volume effects dominate over ideal terms [9]. The reduced osmotic pressure in the reservoir can be written as $\Pi\langle N\rangle_0/kT\rho_0 = 1 + x/2$ [8,9], where the first term represents the ideal van 't Hoff law, and the second the excluded-volume contributions.

The order parameter $g(z)$ contains all information on the structure of the confined solution, e.g., the density profile of chain ends, $2\rho_0 g(z)/\langle N\rangle_0$, the density profile of segments, $\rho(z) = \rho_0 g(z)^2$, and the average degree of polymerization in the gap, $\langle N\rangle = \langle N\rangle_0 \int_0^D g(z)^2\,dz / \int_0^D g(z)\,dz$.

We follow de Gennes in taking the effects of the segment-surface interactions into account by the boundary condition $dg(z)/dz = -cg(z)$ at $z = 0$ and $dg/dz = cg$ at $z = D$, where c^{-1} is the adsorption or extrapolation length, which quantifies the affinity between polymers and surface (the stronger the affinity the larger c) [27]. $c \to -\infty$ implies that the surface acts as a perfectly repulsive hard surface for the segments. $c = 0$ marks the crossover towards positive adsorption.

In this paper we pay particular attention to the regime of *strong confinement*, occurring when the extrapolation length $|c^{-1}|$ exceeds the gap width D. Then the profile $g(z)$ can be taken to be homogeneous ("flat-profile approximation") [1]. Integrating Eq. (1) over the confined volume, and applying the Gauss theorem and the boundary condition, the resulting volume integral of the left-hand side of Eq. (1), $\int(d^2g(z)/dz^2)\,dV$, is substituted by the surface integral $\int(dg(z)/dz)\,dS$, which equals $2Acg$ according to the above-mentioned boundary condition. In the right-hand side of Eq. (1), g is assumed to be constant across the gap and equal to the value at the surface. Equation (1) then reduces to

$$xg^3 + \psi g - 1 = 0, \tag{2}$$

where $\psi = 1 - x - 2R_0^2 c/D$. The physically relevant (i.e., positive and real) solution is $g = \eta/(6x) - 2\psi/\eta$, where $\eta = x^{2/3}\left(108 + 12\sqrt{3}\sqrt{(4\psi^3 + 27x)/x}\right)^{1/3}$ [1]. From the expression for the relation between $g(z)$ and the mean chain length, we see immediately that $g = \langle N\rangle/\langle N\rangle_0$. Note that it is assumed that $g(z)$ is constant, whereas at the same time cases for which $c \neq 0$ are considered. This may seem somewhat counterintuitive, but comparison with full numerical results confirms that this is correct, and that a large error is made when the above-mentioned surface integral is neglected [8].

Seeking the analogy with other models for the second-order phase transition, it is seen that Eq. (2) sets the minima of the potential

$$U(g) = x\frac{g^4}{4} + \psi\frac{g^2}{2} + hg \tag{3}$$

with $h = -1$. This expression has the form of a Landau potential for the order parameter g under external field h. If h would vanish, this would reduce to the Landau potential which yields the second-order transition at $\psi = \psi_c \equiv 0$ [6]. Examining the nonconfined case ($D \to \infty$), we see that the critical value of x, for which $\psi = \psi_c$, is 1 [$x_c(\infty) = 1$]. Confinement shifts the critical value of x, and at the transition, $\psi = 0$, we obtain $[x_c(D) - x_c(\infty)]/x_c(\infty) = -2R_0^2 c/D$. The expression for $x_c(D)$ has the same structure as the one for the transition temperature of superconducting films as analyzed in Ref. [5]. In the present expression, for living polymers R_0 is the radius of gyration of the average chain in the reservoir, and in the case of superconductivity R_0 plays the role of the superconducting coherence length. For living polymers, $x_c(D)$ can be both larger and smaller than $x_c(\infty)$, depending on the sign of c.

The Landau potential $U(g)$ with the order parameter g and $h = 0$ describes the classical second-order transition. When $\psi < 0$, the order parameter is nonzero, implying that chains are present between the two surfaces. But when $\psi \geqslant 0$, the order parameter is zero. This is illustrated by the dashed red curves of Fig. 1.

With a fixed value for the "external field," $h = -1$, such as arises from Eq. (1) for confined living polymers in equilibrium with a reservoir solution, the transition will be more gentle (solid black lines in Fig. 1). Differentiating Eq. (2) twice, we see that $g(\psi)$ exhibits an inflection at $\psi = \psi_c$. This inflection is what remains of the second-order transition when $h = -1$. We refer to this "rudiment" of the second-order transition as a "near-second-order transition," especially for those cases where it still corresponds to a large change of properties such as $\langle N\rangle$, $\langle\rho\rangle$, and Ω^d of the confined solution, upon a small change of control parameters such as, e.g., D or x.

From Eq. (2) it is seen readily that the crossover from positive adsorption ($g > 1$) to depletion ($g < 1$) occurs at $\psi = 1 - x$. This implies that at any nonzero R_0 and finite D this crossover occurs at $c = 0$, as expected. Hence, for $x = 1$ the crossover from adsorption to depletion coincides with the near-second-order transition. It is also seen immediately from Eq. (2) that at the transition ($\psi = 0$) the order parameter scales as $g = x^{-1/3}$. Thus, for $x < 1$ the transition occurs in the adsorption regime, as for $g > 1$ the segment concentration inside the gap between the surfaces exceeds that in the reservoir. For $x = 0$ there is a true second-order transition at $\psi = 0$, at which g and hence the segment concentration in the gap diverge [10]. For $x > 1$, we see that the transition occurs in the depletion regime, as $g < 1$ at the transition, implying that the segment concentration in the gap is smaller than in the reservoir. All this is illustrated in Fig. 1, which

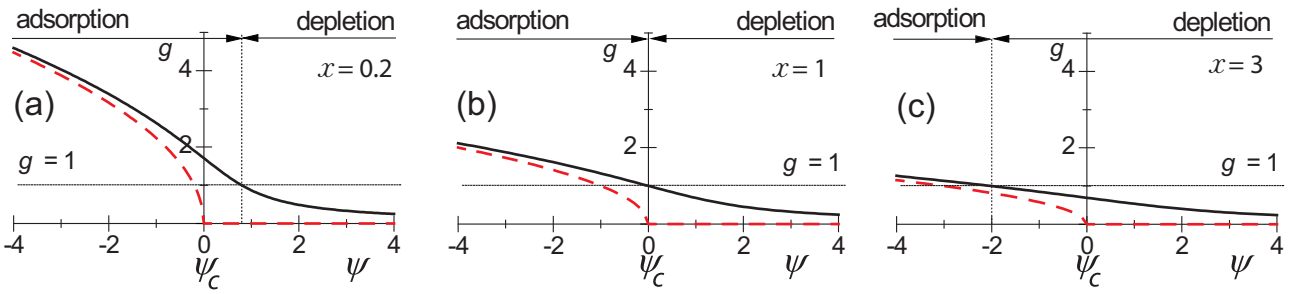

FIG. 1. Transition of g [global minimum of the potential $U(g)$] for different values of the parameter x and the "external field" h: $h = 0$ (dashed red curves), $h = -1$ (solid black curves). The critical value of $\psi, \psi_c \equiv 0$ is defined by $d^2g/d\psi^2 = 0$.

shows the development of the position of the minimum of potential $U(g)$ with ψ at different values of the parameters x, for $h = 0$ and $h = -1$. At $h = 0$ the second-order transition is clearly notable at $\psi = 0$. Whereas for the living-polymer system at equilibrium with a reservoir, which implies that $h = -1$, condition $\psi = 0$ refers to a "near-second-order transition" showing up as an inflection. For the dilute reservoir, which implies that $x < 1$, the transition occurs at adsorbing conditions ($c > 0$, hence $g > 1$). For a marginal polymer solution in the reservoir ($x > 1$) the transition takes place when $c < 0$ (depletion) and therefore $0 \leqslant g < 1$.

To finalize this section, we consider solutions of Eq. (2) in the limit of small distances. When $D \to 0$ then $\psi \to -\infty$ for adsorbing surfaces ($c > 0$), and $\psi \to \infty$ for depleting surfaces ($c < 0$). Asymptotic solutions for these cases are easily obtained because both limits are far from ψ_c. For $\psi \to \infty$ (depleting surfaces), g becomes small, and the nonlinear term in Eq. (2) becomes negligible. Then $g \simeq 1/\psi$, and the average degree of polymerization in the gap between the surfaces vanishes as $\langle N\rangle \simeq -\langle N\rangle_0 D/(2R_0^2 c)$. For $\psi \to -\infty$ (adsorbing surfaces) the term -1 in Eq. (2) is negligible. Then we obtain $g \simeq \sqrt{-\psi/x}$, and the average degree of polymerization diverges as $\langle N\rangle \simeq \langle N\rangle_0 (2R_0^2 c/(xD))^{1/2}$ [1]. We see that at small surface separations D, the scaling law for $\langle N\rangle$ is just controlled by the polymer surface affinity.

The analysis in this paper is based on a mean-field approximation at the level of the second virial coefficient among segments (= excluded-volume parameter). As clarified by Schaefer in Ref. [28] and reviewed, e.g., in Chap. 1 of Ref. [29], it is known that a mean-field description of polymers in solution works well in certain regimes, such as the ideal-dilute and marginal regimes, but exhibits deviations in others. The mean-field approximation accounts for a crossover between the dilute and the marginal regime, which is in our symbols given by $x = 1$. Within the mean-field approximation the nonideal dilute and semidilute regimes are not described correctly. So, when either the reservoir phase or (local concentrations in) the confined phase or both fall in the later "non-mean-field" regimes, deviations are to be expected. The qualitative behavior will be similar as predicted, but scaling exponents may deviate. The importance of the non-mean-field regime depends on the chain stiffness and is significant especially for very flexible chains. For the highest concentrations, higher-order interactions, beyond the second virial coefficient among segments, give rise to the concentrated regime. Owing to these higher-order interactions, (local) segment concentrations ρ (and hence also g) will in practice be restricted by a close-packing upper bound.

III. CONNECTION WITH EXPERIMENT

To connect with experiment, we now focus on interactions between surfaces immersed in solutions of living polymer. The contributions owing to the living polymers to these surface interactions reflect the structure and properties of the living polymers confined between the surfaces. For plan-parallel surfaces these interactions can be quantified in terms of the so-called disjoining potential Ω^d per unit area, or the disjoining pressure $p^d = -\partial\Omega^d/\partial D$, where D is the distance between the surfaces. The relation between theoretical predictions for plan-parallel surfaces and experimental systems involving curved surfaces is made by the Derjaguin relation [30,31], which states that for distances that are considerably smaller than the radii of curvature of the surfaces, the disjoining potential per unit area Ω^d between two planar surfaces is proportional to the normalized disjoining force F^d/R between curved surfaces with characteristic radius R. The proportionality constant depends on the nature of the curvature of the surfaces involved (e.g., cylindrical, spherical). In colloidal systems such surface interactions are crucial because the interaction between particle surfaces determines the behavior of colloidal systems as a whole. Furthermore, these forces can be experimentally investigated by a surface force balance or by CP AFM [25,26]. Such surface-interaction experiments may be utilized to experimentally investigate the near-second-order transition for living-polymer solutions in confinement. In superconductivity experiments, the film thickness is fixed and temperature is the control parameter in measuring the film conductivity. In the case of living-polymer solutions, the distance between the confining surfaces is readily varied in, e.g., a CP AFM experiment, while the polymer excluded-volume parameter (analog of temperature for the superconductivity case) is fixed. Therefore, the disjoining potential between planar surfaces will be carefully examined in this second part of the paper.

The influence of the confining surfaces upon the confined solution is reflected by an interaction between the surfaces, which can be quantified in terms of the disjoining potential per unit area, $\Omega^d \equiv \Omega^\sigma(D) - \Omega^\sigma(\infty)$, where $\Omega^\sigma(D) \equiv \Omega + \Pi D$ denotes the interfacial excess grand potential per unit area. Ω is the grand potential per unit area and Π is the osmotic pressure at equilibrium. It can be expressed in terms of the equilibrium

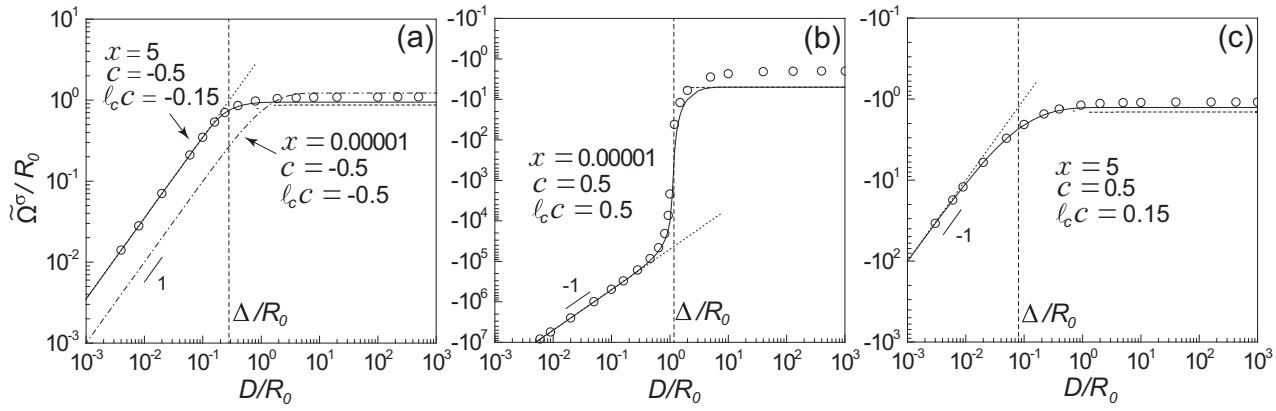

FIG. 2. The normalized interfacial excess grand potential versus normalized gap width for three sets of parameters at $\ell_c|c| < 1$. Solid and dash-dotted curves denote the exact solution of Eq. (1) with Eq. (4), and open circles show the flat-profile approximation, Eq. (2) with Eq. (6). Dotted lines represent the small-distances asymptotic, Eqs. (7), and dashed lines represent the result obtained with Eq. (10). The vertical dashed line at Δ/R_0 indicates the crossover distance from strong to almost no interference between surfaces. (a) Depletion ($c < 0$), (b) near-second-order transition (small x, positive c), and (c) positive adsorption from a marginal solution.

segment-concentration profile as [1]

$$\widetilde{\Omega}^{\sigma}(D) = \int_0^D (1-\widetilde{\rho}(z))\,dz + \frac{x}{2}\int_0^D (1-\widetilde{\rho}(z)^2)\,dz, \quad (4)$$

where for brevity, $\widetilde{\Omega}^{\sigma}(D) \equiv \Omega^{\sigma}(D)\langle N\rangle_0/(\rho_0 kT)$ and $\widetilde{\rho}(z) \equiv \rho(z)/\rho_0$ is the solution of Eq. (1) with $\widetilde{\rho}(z) = g(z)^2$.

A selection of results for $\widetilde{\Omega}^{\sigma}(D)$ is shown in Fig. 2. Results based on the exact numerical solution of Eq. (1) are indicated by solid and dash-dotted lines for four sets of parameters. The sets are chosen to cover possible experimental scenarios for ideal and marginal solutions confined by slight segment repelling [$c \lesssim 0$, Fig. 2(a)] and segment adsorbing [$c \gtrsim 0$, Figs. 2(b) and 2(c)] surfaces. It is obvious to introduce the characteristic length scale, Δ, which delimits two different gap-width behaviors, namely, $\Delta \ll D$, where the layers adjoining the surfaces do not interfere with each other, and $D \ll \Delta$, where they do.

When polymer solutions between adsorbing surfaces are nearly ideal (more generally at $0 \leqslant x \leqslant 1$), Fig. 2(b), Δ is the value of D at which the near-second-order transition takes place at $\psi = 0$. Simple algebra provides the expression

$$\Delta = 2\frac{R_0^2 c}{1-x}. \quad (5)$$

Notice that to keep the value of Δ finite and positive for x in close proximity of 1, $|c|$ should be negligibly small.

When two surfaces are far apart, so that surface layers do not interfere ($D > \Delta$), the interfacial excess grand potential is controlled by the affinity of monomers to the single surface and is independent of the distance D. The expression for $\widetilde{\Omega}^{\sigma}(D)$ at large distances can be calculated from Eq. (4) using the expression for the segment density profile at single surfaces obtained by van der Gucht *et al.* [9].

For small distances, the combined effect of two surfaces on segments is large, and the segment density in the gap is close to homogeneous, and described well by the "flat-profile expression," Eq. (2). For such a homogeneous profile Eq. (4) simplifies to

$$\widetilde{\Omega}^{\sigma}(D) = \left(1 + \frac{x}{2} - \widetilde{\rho} - \frac{x}{2}\widetilde{\rho}^2\right)D, \quad (6)$$

where $\widetilde{\rho} \equiv \rho/\rho_0 = g^2$ with g the solution of Eq. (2). Results of Eq. (6) are shown in Fig. 2 by circles. We see that at $D < \Delta$, the flat-profile approximation coincides with the results of the exact numerical solution of Eq. (1).

If the surface repels polymers, $c < 0$, the gap is nearly empty at small distances and $\widetilde{\rho} \simeq 0$ in Eq. (6). In the case of polymer-attracting surfaces, $c > 0$, the effect of surfaces is large at small distances and g becomes also large. The contribution -1 in Eq. (2) can then be neglected and therefore $\widetilde{\rho} \simeq -\psi/x \simeq 2R_0^2 c/xD$ [1]. Thus for the adsorbing and depleting surfaces at small D, Eq. (6) reduces to

$$\widetilde{\Omega}^{\sigma}(D) \simeq \begin{cases} \left(1+\frac{x}{2}\right)D & \text{if} \quad c<0, \quad D<\Delta, \\ -\frac{2R_0^4 c^2}{xD} & \text{if} \quad c>0, \quad D<\Delta. \end{cases} \quad (7)$$

In the expression for $c < 0$ we recognize the reduced osmotic pressure of the reservoir solution times the distance, as it should be for depletion interaction. Dotted lines in Fig. 2 are from Eqs. (7). At small distances these coincide with the full numerical results. At large D, the density profile cannot be considered flat anymore, and the effect of the inhomogeneity becomes significant.

Indeed, for large distances between surfaces, the flat-profile approximation is not precise in estimating the interfacial excess grand potential. However, it is worthwhile to calculate $\widetilde{\Omega}^{\sigma}(\infty)$ assuming that the mean segment concentration inside the gap is about the same as its value in the reservoir. Linearizing Eq. (2) around $g = 1$ we obtain $\widetilde{\rho} \simeq [1 + 2c/(D(1+2x)/R_0^2 - 2c)]^2$, and after substitution into Eq. (6) and taking $D \to \infty$, the interfacial excess grand potential reads

$$\widetilde{\Omega}^{\sigma}(\infty) \simeq -4\ell_c^2 c(1+x), \quad (8)$$

where the correlation length $\ell_c = R_0/\sqrt{1+2x}$ characterizes the length scale of the profile decay towards reservoir density

ρ_0, as defined in Ref. [21]. The appearance of the correlation length ℓ_c in Eq. (8), which assumes homogeneous profiles, indicates its origin coming from the inhomogeneous profile. Direct use of Eq. (6) with $\widetilde{\rho} = 1$ gives $\widetilde{\Omega}^{\sigma}(\infty) = 0$. This is valid only at $c = 0$. Only then the segment concentration profile is truly flat. Somewhat counterintuitively, the "flat-profile approximation" introduced with Eq. (2) does account for certain consequences of profile inhomogeneity, as, e.g., reflected in Eq. (8). Below we consider the transition from an inhomogeneous to a flat distribution of monomers to establish conditions when Eq. (8) holds.

In the limit of weak adsorption or depletion, Eq. (1) can be linearized by substituting $g(z) = 1 + \delta(z)$. This yields a second-order linear differential equation for $\delta(z)$. For large gap widths, $D \gg \ell_c$, the equation provides the segment density profile

$$\widetilde{\rho}(z) = \left[1 + \frac{\ell_c c}{1 - \ell_c c}\left(e^{-\frac{z}{\ell_c}} + e^{\frac{z-D}{\ell_c}}\right)\right]^2. \tag{9}$$

This expression is valid at $|\ell_c c/(1 - \ell_c c)| \leqslant 1$ to keep $|\delta(z)| < 1$. The profile may be considered homogeneous for values of c small enough to ensure $\ell_c c \ll 1$.

After substitution of Eq. (9) into the expression for the interfacial excess grand potential, Eq. (4), the potential for two infinitely separated surfaces becomes

$$\widetilde{\Omega}^{\sigma}(\infty) = -\frac{\ell_c^2 c(4 - 3\ell_c c)}{(1 - \ell_c c)^2} - \frac{x}{12}\frac{\ell_c^2 c\left(48 - 108\ell_c c + 88\ell_c^2 c^2 - 25\ell_c^3 c^3\right)}{1 - 4\ell_c c + 6\ell_c^2 c^2 - 4\ell_c^3 c^3 + \ell_c^4 c^4}. \tag{10}$$

The above expressions reveal a reduced scale $\ell_c c$. At small $\ell_c|c|$ ($\ll 1$), the potential reduces to Eq. (8) found from the flat-profile approximation. The result for $\widetilde{\Omega}^{\sigma}(\infty)$ calculated from Eq. (10), which assumes a slightly inhomogeneous profile, is shown in Fig. 2 by dashed lines. They are quite close to the exact result. Equations (8) and (10) predict slightly different values, when the value of $\ell_c c$ is not small enough.

The typical range of the interaction is quantified by the crossover distance Δ, where the small-distance scaling law for $\widetilde{\Omega}^{\sigma}(D)$ intersects with the level $\widetilde{\Omega}^{\sigma}(\infty)$. The small-distance scaling for $\widetilde{\Omega}^{\sigma}(D)$ is given by Eqs. (7), whereas $\widetilde{\Omega}^{\sigma}(\infty)$ is obtained from solution of Eq. (1) for a single surface [9]. For weak adsorption or depletion $\widetilde{\Omega}^{\sigma}(\infty)$ is approximated well with Eq. (10). However, as shown above, in the case of the

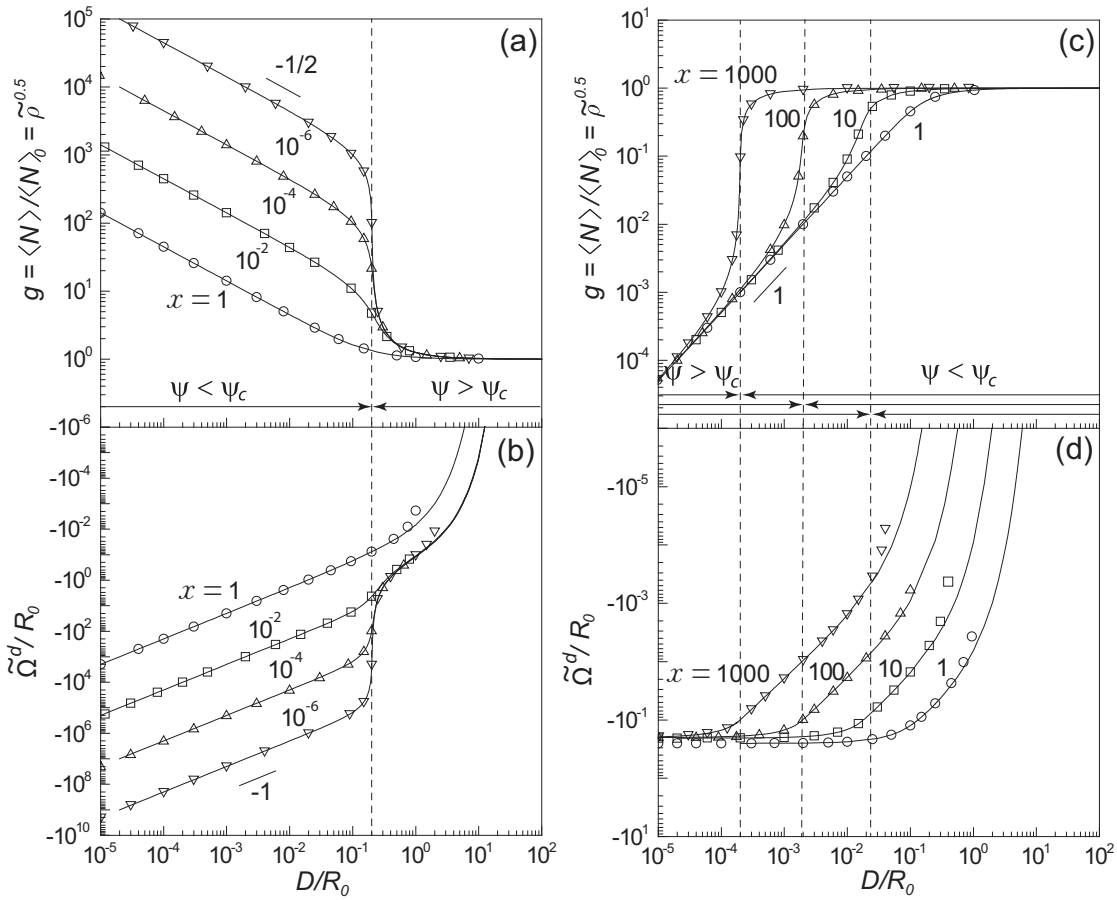

FIG. 3. The average degree of polymerization, $\langle N\rangle$, and the reduced disjoining potential Ω^d for different excluded-volume parameter x (indicated near the curves) and affinity of segments to surfaces: (a, b) $c = 0.1$, (c, d) $c = -0.1$. Solid curves show numerical solution, and symbols are the solution of Eqs. (2) and (6). The near-second-order transition, $\psi = \psi_c \equiv 0$, is denoted by dashed vertical lines for given values of x. The sign of ψ is indicated by horizontal arrows.

near-second-order transition, Δ does not depend on the interfacial excess grand potential of the surface at infinite separation. For all other conditions, this dependency can be traced. For living polymers in depleting conditions at any value of x, the first equation from the set of Eqs. (7) provides

$$\Delta = \frac{\widetilde{\Omega}^{\sigma}(\infty)}{1 + x/2}. \tag{11}$$

Hence, in the limit of small $|c|$ for depleting surfaces, the crossover distance Δ scales with c as $-4\ell_c^2 c(1 + x)/(1 + x/2)$. For strong depletion, $c \to -\infty$, Δ levels off to $\ell_c(3 + 25x/12)/(1 + x/2)$ according to the flat-profile approximation for the segment distribution between surfaces.

For marginal solutions ($x > 1$) confined between adsorbing surfaces ($c > 0$), the second equation of the set of Eqs. (7) yields

$$\Delta = -2\frac{R_0^4 c^2}{x\widetilde{\Omega}^{\sigma}(\infty)}. \tag{12}$$

Although all the three expressions [Eqs. (5), (11), and (12)] for the crossover distance differ from each other, in the limit of $\ell_c|c| \ll 1$, we obtain the master scaling $\Delta = \alpha\ell_c^2 c$ with α as a factor depending on x and c. As an example, for a near-ideal solution confined by slightly attractive surfaces, Eq. (5) yields $\alpha = 2(1 + 2x)/(1 - x)$, and in the regime of ideal solution, $\Delta \simeq 2R_0^2 c$. Equations (8) and (10) are quite accurate if $|\widetilde{\Omega}^{\sigma}(\infty)/R_0| < 1$.

Figure 3 reports the effect of confinement on the living polymer solution for different values of x. The top and bottom panels refer to the mean degree of polymerization inside the gap, g, and the disjoining potential between surfaces, $\Omega^d(D)$, respectively. Particular attention is paid to the cases where the confined solution undergoes a pronounced near-second-order transition at $\psi = \psi_c$, as g undergoes a large change upon a small variation of the distance between surfaces. For adsorbing surfaces [Figs. 3(a) and 3(b)], the change of $\langle N\rangle$ and $\widetilde{\Omega}^d \equiv \Omega^d\langle N\rangle_0/(\rho_0 kT)$ is quite pronounced for $x < 1$. The order parameter for small distances (where $\psi < 0$) scales as predicted above: $\langle N\rangle \simeq \langle N\rangle_0(2R_0^2 c/(xD))^{1/2}$. Because of the large excess of confined monomers at $D < R_0$ and $c > 0$, and the small value of $\widetilde{\Omega}^{\sigma}(\infty)$, the excess grand potential and the disjoining potential follow Eqs. (7): $\widetilde{\Omega}^d(D) \simeq \widetilde{\Omega}^{\sigma}(D) \simeq -(R_0^4 c^2)D^{-1}$.

When the solution in the reservoir is marginal ($x \gg 1$) and surfaces are depleting ($c < 0$), the transition at $\psi = \psi_c$ is again revealed by a change of the order parameter g by several orders of magnitude [Fig. 3(c)]. For these low local concentrations of confined monomers, the first term of Eq. (1) is negligible, and hence parameter x has no effect on g. Then, for narrow gaps ($D \ll R_0$) and positive ψ, the order parameter increases linearly with D, $g \simeq -D/(2R_0^2 c)$. For this case, the disjoining potential is constant [Fig. 3(d)]. Thus, for small D, $\widetilde{\Omega}^{\sigma}(D)$ as given by Eq. (7) ($c < 0$) is negligible as compared to $-\widetilde{\Omega}^{\sigma}(\infty)$, so the latter dominates $\widetilde{\Omega}^d(D)$. $\widetilde{\Omega}^{\sigma}(\infty)$ is predicted by Eq. (10). Hence, for small $\ell_c c$, we obtain $\widetilde{\Omega}^d(D) \simeq 4R_0^2 c(1 + x)/(1 + 2x)$, which for large values of x becomes $2R_0^2 c$.

IV. CONCLUSION

For a living-polymer solution strongly confined between two surfaces ($|c|D < 1$), the synergy between the influence of surfaces on the local concentration and the reversible polymerization of the living polymers yields a near-second-order transition inside the gap. As illustrated in Fig. 1, the order parameter g and hence the normalized local monomer concentration $\widetilde{\rho} = g^2$ as a function of the parameter ψ ($\equiv 1 - x - R_0^2 c/D$) decreases from a high value at $\psi \to -\infty$ to zero when $\psi \to \infty$. At the transition, $\psi = \psi_c \equiv 0$. There $g(\psi)$ exhibits an inflection ($d^2\rho/d\psi^2 = 0$). At the crossover from depletion to adsorption $c = 0$ and $g = 1$ so that $\psi = 1 - x$. For dilute solutions ($x < 1$) the transition occurs at adsorbing surfaces only, because $\psi = 0$ implies that for $x < 1$ we get $R_0^2 c/D = 1 - x > 0$, and hence that $c > 0$. The smaller x, the more pronounced the transition, as illustrated in Figs. 3(a) and 3(b). So the transition between adsorbing surfaces is observed most clearly with near-ideal dilute living-polymer solutions ($x \ll 1$). To maximize the interaction distance, e.g., in order to facilitate experimental investigations, a nearly ideal living-polymer solution with a large mean radius of gyration, R_0, in solution should be chosen, together with a small adsorption length, c^{-1} (strong adsorption). For marginal solutions, and solutions even more concentrated than that ($x > 1$), the transition only occurs between depleting surfaces, as $\psi = 0$ implies that for large x, $R_0^2 c/D = 1 - x < 0$, and hence $c < 0$. For such negative c, the transition at ψ_0 is most pronounced at high x values. Because Δ/R_0 is small for this regime, solutions with very large R_0 are required in order to observe the transition experimentally.

When the polymer solution is nearly ideal and confined between adsorbing surfaces, the disjoining potential Ω^d, which quantifies the interaction between surfaces and that can be measured by means of, e.g., CP AFM, clearly reflects the transition: Ω^d experiences a significant sudden decrease upon decreasing the distance between surfaces at the gap width $D = \Delta$ at which $\psi = \psi_c = 0$. However, when a marginal solution is confined by depleting surfaces, Ω^d levels off at small intersurface distances and becomes equal to $-\Omega^{\sigma}(\infty)$.

The interaction distance between surfaces shows a master dependency, $\Delta \equiv \alpha\ell_c^2 c$, where the prefactor α depends on the particular conditions. For cases where the onset of interference between the surface layers of the two confining surfaces does not coincide with a near-second-order transition, one predicts the scaling $\Delta \simeq R_0^2|c|/x$ for marginal, and $\Delta \simeq R_0^2|c|$ for nearly ideal, solutions. Similar scaling laws can be derived directly from $\psi = 0$, indicating that the surface separation at which the transition occurs scales in the same way with ℓ_c and c. Summarizing, $\ell_c^2|c|$ is the length scale of the range of the solution mediated surface interactions.

ACKNOWLEDGMENTS

This work was supported by ECHO Grant No. 700.59.025 from the Netherlands Organization for Scientific Research (NWO).

[1] N. A. M. Besseling and A. V. Korobko, Phys. Rev. Lett. **111**, 186103 (2013).
[2] H. W. Diehl, Int. J. Mod. Phys. B **11**, 3503 (1997).
[3] K. Binder and P. C. Hohenberg, Phys. Rev. B **6**, 3461 (1972).
[4] H. Nakanishi and M. E. Fisher, J. Chem. Phys. **78**, 3279 (1983).
[5] D. G. Naugle and R. E. Glover, Phys. Lett. A **28**, 110 (1968).
[6] L. D. Landau and E. M. Lifshitz, *Statistical Physics*, 3rd ed. (Butterworth-Heinemann, Washington, DC, 1980).
[7] P. G. de Gennes, *Superconductivity of Metals and Alloys* (Benjamin, New York, 1966).
[8] A. V. Korobko and N. A. M. Besseling (unpublished).
[9] J. van der Gucht, N. A. M. Besseling, and G. J. Fleer, Macromolecules **37**, 3026 (2004).
[10] J. van der Gucht, N. A. M. Besseling, and G. J. Fleer, J. Chem. Phys. **119**, 8175 (2003).
[11] L. Brunsveld, B. J. B. Folmer, E. W. Meijer, and R. P. Sijbesma, Chem. Rev. **101**, 4071 (2001).
[12] M. J. Serpe and S. L. Craig, Langmuir **23**, 1626 (2007).
[13] T. F. A. de Greef, G. Ercolani, G. B. W. L. Ligthart, E. W. Meijer, and R. P. Sijbesma, J. Am. Chem. Soc. **130**, 13755 (2008).
[14] F. C. Mackintosh, S. A. Safran, and P. A. Pincus, Europhys. Lett. **12**, 697 (1990).
[15] M. E. Cates and S. J. Candau, J. Phys. Condens. Matter **2**, 6869 (1990).
[16] T. D. Pollard and J. A. Cooper, Annu. Rev. Biochem. **55**, 987 (1986).
[17] A. V. Tobolsky and W. J. MacKnight, *Polymeric Sulphur and Related Polymers* (Interscience, New York, 1965).
[18] Y.-Y. Won, H. T. Davis, and F. S. Bates, Science **283**, 960 (1999).
[19] M. E. Cates, J. Phys. **49**, 1593 (1988).
[20] T. F. A. de Greef, M. M. G. Smulders, M. Wolffs, A. P. H. J. Schenning, R. P. Sijbesma, and E. W. Meijer, Chem. Rev. **109**, 5687 (2009).
[21] J. van der Gucht, N. A. M. Besseling, and M. A. Cohen Stuart, J. Am. Chem. Soc. **124**, 6202 (2002).
[22] C. E. Woodward and J. Forsman, Macromolecules **42**, 7563 (2009).
[23] C. E. Woodward and J. Forsman, J. Chem. Phys. **133**, 154902 (2010).
[24] M. E. Helgeson and N. J. Wagner, J. Chem. Phys. **135**, 084901 (2011).
[25] W. A. Ducker, T. J. Senden, and R. M. Pashley, Nature (London) **353**, 239 (1991).
[26] W. Knoben, N. A. M. Besseling, and M. A. Cohen Stuart, Phys. Rev. Lett. **97**, 068301 (2006).
[27] P. G. de Gennes, Rep. Prog. Phys. **32**, 187 (1969).
[28] D. W. Schaefer, Polymer **25**, 387 (1984).
[29] G. J. Fleer, M. A. Cohen Stuart, J. M. H. M. Scheutjens, T. Cosgrove, and B. Vincent, *Polymers at Interfaces*, 1st ed. (Chapman and Hall, London, 1993).
[30] B. V. Derjaguin, Kolloid Zh. **69**, 155 (1934).
[31] J. N. Israelachvilli, *Intermolecular and Surface Forces*, 3rd ed. (Academic Press, New York, 2011).